BEYOND 1 SUN: EVALUATING THE EFFICIENCY OF AGED P-TYPE PERC AND N-TYPE TOPCON SILICON DEVICES UNDER HIGH-IRRADIANCE CONDITIONS

Marília Braga, Ana Carolina O. Machado, Ícaro E. da Cunha, Anelise M. Pires, Helena F. Naspolini, Ricardo Rüther

Universidade Federal de Santa Catarina, Fotovoltaica/UFSC, Florianópolis (Brazil)

Abstract

Single-junction photovoltaic devices are nearing their efficiency limits, making second-order effects increasingly relevant. In high-sun regions such as Brazil, irradiance frequently exceeds 1 sun, yet device performance under these conditions remains insufficiently characterized. This work evaluates aged p-type PERC and n-type TOPCon minimodules using outdoor measurements on a single-axis tracker and controlled indoor tests. Prior to testing, all samples were subjected to 1000 hours of damp-heat aging following IEC 61215. The site's irradiance distribution shows that more than one quarter of the total incident energy occurs at or above 1000 W/m². Both indoor and outdoor measurements reveal efficiency losses at elevated irradiance, primarily driven by series resistance effects. Under these conditions, the aged PERC samples in this work exhibit stronger degradation and more pronounced fill-factor reductions compared to the TOPCon samples. The TOPCon samples in this study maintain greater stability under increasing irradiance, which may be associated with differences in degradation pathways and series resistance evolution rather than intrinsic technology advantages alone. By combining irradiance-dependent performance with the local energy distribution, global weighted efficiencies indicate that the studied TOPCon samples adapted more effectively to high-irradiance conditions, translating this into higher operating efficiency. These results emphasize the need to characterize PV technologies beyond STC and highlight that minimizing series resistance—particularly after aging—is critical for optimizing performance in high-irradiance climates.

Keywords: PV Efficiency, Device Optimization, Irradiance Response, Over-Irradiance, Indoor Characterization, Outdoor Performance.

1. Introduction

The pursuit of higher photovoltaic (PV) efficiencies has pushed crystalline silicon (c-Si) technologies closer to their theoretical limits. With the current record for silicon single-junction cells reaching 27.3% dating back to 2023 (NREL, 2025)— just 5 percentage points below the 32.3% Shockley–Queisser limit (Shockley and Queisser, 1961)— further gains demand attention to subtle loss mechanisms. Among these, resistive and optical losses in front metallization become more critical as current levels rise with increasing irradiance.

Standard test conditions (STC), defined at 1000 W/m² (also known as 1 sun) for irradiance, do not encompass the full spectrum of real-world operating conditions. In climates such as Brazil's, over-irradiance events—where irradiance exceeds extraterrestrial values—are frequent and significant. Measurements in locations with high solar resource and dynamic cloud conditions, like Florianópolis, have recorded irradiance peaks up to 1845.5 W/m² (Martins et al., 2022). These events often go undetected in low-resolution datasets but can influence both performance and component reliability, contributing to phenomena such as fuse failures and underestimated inverter clipping losses (Braga et al., 2020; Nascimento et al., 2019).

Beyond reliability concerns, these events also represent an underexplored opportunity for performance optimization. While the low-light response of PV modules is a well-understood phenomenon, the behavior of modules under irradiance levels exceeding 1000 W/m² remains largely unexamined. As irradiance increases, so does photocurrent, leading to higher resistive losses. Optimizing the layout and thickness of busbars and fingers thus becomes even more relevant under high-irradiance conditions. However, this design trade-off between shading and resistive losses of metallization is typically optimized for STC, since module efficiency under STC is the basis for pricing of PV modules. No experimental studies could be identified in the literature that validate or quantify module performance under over-irradiance; only simulated efficiencies have been reported (Queiroz et al., 2022). This is particularly relevant for high-irradiance climates such as Brazil's, where some sites have recorded over 30% of the total incident energy occurring at or above 1000 W/m² (Queiroz et al., 2022).

10.18086/swc.2025.03.09 Available at http://proceedings.ises.org

To address this gap, this work evaluates the efficiency of p-type PERC (Passivated Emitter and Rear Cell) and n-type TOPCon (Tunnel Oxide Passivated Contact) silicon devices under over-irradiance, both indoors—using an LED solar simulator—and outdoors under natural sunlight. Given the dependence of long-term yield on aged behavior, the minimodules were pre-aged (1000 h damp-heat at 85 °C/85 % relative humidity; IEC 61215) before testing to emulate field-relevant degradation (IEC, 2021a). The objective is to characterize and compare their response across a wide irradiance range and quantify the real-world impact relative to STC expectations, enabling incorporation of any deviations into energy-yield simulations and informing design choices for sunny regions prone to over-irradiance—where meaningful energy may lie beyond the conventional "1 sun" paradigm.

2. Methodology

2.1. Samples

Six custom minimodules were installed in the outdoor setup. This work reports results for four representative units: (i) two M10 n-type TOPCon devices consisting of two series-connected half-cells each, and (ii) two G12 p-type PERC devices with two series-connected half-cells each. Immediately after fabrication, all six minimodules underwent 1000 h of damp-heat at 85 °C/85 % relative humidity in accordance with IEC 61215-1 (IEC, 2021a). Following the damp heat test, baseline performance was verified on the indoor setup, and the devices were then installed outdoors on 7 March 2025 and continuously monitored until 30 September 2025.

2.2. Outdoor Experimental Setup

The experimental setup is installed at the Fotovoltaica-UFSC laboratory in Florianópolis, Brazil (27.4°S, 48.4°W). The setup includes a versatile outdoor single-axis tracker (SAT) test bench with electronic loads and environmental sensors that enable the characterization of PV modules and cells under real operating conditions (Figure 1). IV curves are acquired every minute using four-wire measurements to avoid minimize measurement errors related to cable resistive losses and voltage drops. The loads operate in various modes, including MPPT, voltage bias, open circuit, and short circuit. Two different load types are used in the experimental setup: high-power units with active cooling for PV modules up to 900 W, and low-power units with passive dissipation for devices up to 300 W, such as minimodules or cells. All units are customized for improved accuracy in their respective current and voltage ranges. Measurement uncertainty depends on the load temperature, with maximum errors of 0.3% in current and 0.2% in voltage. Minimodule samples used in this study are mounted on an acrylic support plate with weatherproof fixtures that minimize stress and allow easy removal for post-exposure analyses, such as electroluminescence imaging.

Figure 1: Outdoor measurement setup on a single-axis tracker at the Fotovoltaica/UFSC Research Laboratory in Florianópolis, Brazil (27.4°S, 48.4°W), showing the silicon PV minimodules and sensors used in this study.

Irradiance on the plane of the samples is monitored using class A pyranometers, photodiodes, and spectroradiometers. These instruments enable precise broadband irradiance measurements, the detection of irradiance fluctuations and spectral mismatch corrections. Environmental parameters, including temperature, humidity, and wind speed, along with device operating temperature, are continuously recorded. These measurements allow for isolating the impact of irradiance levels on module efficiency. Further details of the outdoor measurement setup are described by (Braga et al., 2024).

All outdoor IV curves were processed according to procedure 4 of IEC 60891:2021 (IEC, 2021b), applying temperature correction to 25 °C across all measured irradiance levels. In addition, the plane-of-array irradiance values were spectrally corrected by considering the integral of the spectral response curves of both the reference sensor and the tested sample, minimizing discrepancies arising from spectral effects. The series resistance (Rs) of each curve was calculated as indicated in the IEC 60891:2021 procedure, while the short-circuit current (Isc) and open-circuit voltage (Voc) were obtained by interpolating or extrapolating each measured IV curve.

It is noted, however, that the standard recommends applying this correction procedure only within the 300–1200 W/m² irradiance range, where the corrected results—such as Isc and Rs—showed behavior more consistent with the expected trend. Outside this range, greater dispersion in the corrected values was observed, which should be interpreted with caution.

2.3. Indoor Characterization

To complement the outdoor measurements, an indoor laboratory is also employed for controlled testing. A solar simulator with an illuminated area of 240 mm × 240 mm is used to validate field measurements, characterize minimodules, and perform stability and degradation tests under defined irradiance and spectral conditions (WAVELABS SINUS-300 Advanced; Figure 2). The simulator operates up to 1.8 suns and allows spectral tuning to better match the Brazilian solar resource or apply stress via UV-rich spectra. Rated Class A++/A/A+ per IEC 60904-9:2020 (IEC, 2020), the unit measures within the 20 V / 16 A range, matching the operating conditions of the two half-cell minimodules.

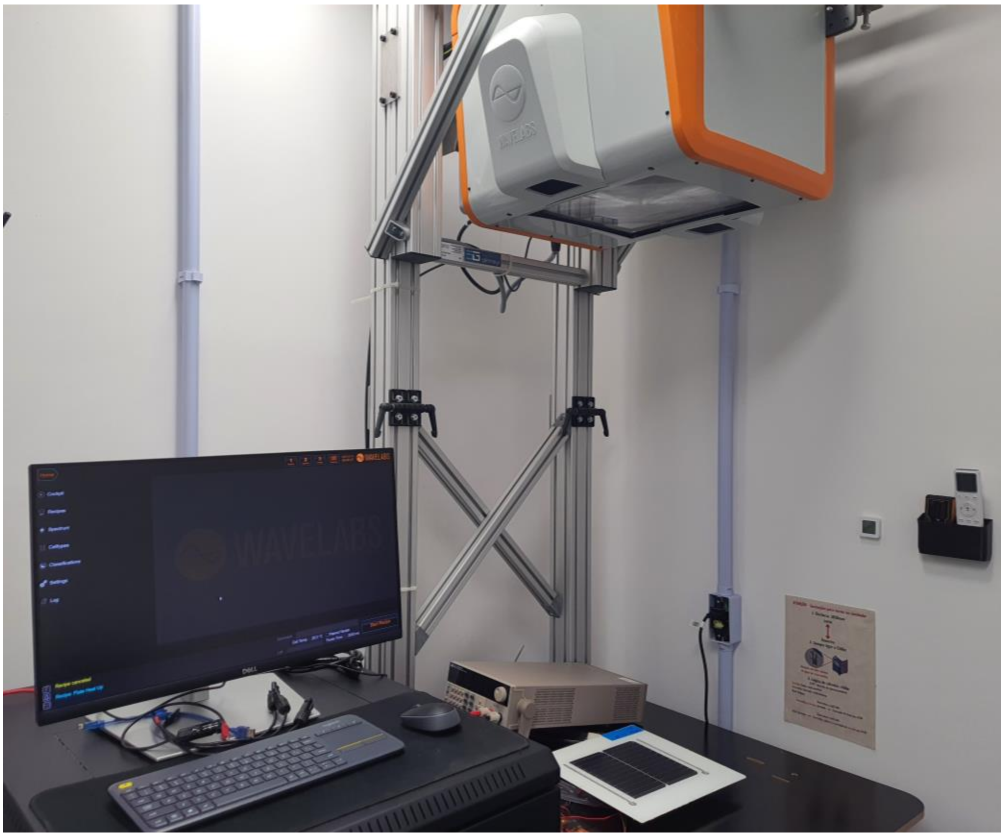

Figure 2: Indoor setup and solar simulator used for controlled irradiance tests at the Fotovoltaica/UFSC Research Laboratory in Florianópolis, Brazil (27.4°S, 48.4°W).

The indoor measurements were conducted under closely monitored and controlled conditions, with a maximum temperature variation of ±1 °C. The measured irradiance was also spectrally corrected, considering the integral of the spectral response curves of the reference sensor and the tested sample, ensuring comparability between measurements under different irradiance levels.

The short-circuit current (Isc) and open-circuit voltage (Voc) were obtained by linear interpolation between two adjacent points of the IV curve, using the two points immediately before and after the intersection with the current and voltage axes, respectively. The resulting Isc value was used to calculate the series resistance (Rs) following the method described in IEC 60891:2021, although procedure 4 was not applied, since the temperature remained stable throughout all measurements.

The device efficiency was determined directly from the current–voltage data at each irradiance step, as the ratio between the maximum electrical power output and the incident optical power on the illuminated area. This analysis allowed correlating resistive losses with the efficiency variation under different irradiance levels.

2.4. Data Analysis and Global Efficiency

The dual setup—dynamic outdoor tests and indoor precision evaluations—provided a comprehensive view of device behavior across operating scenarios. IV curves were recorded under varying irradiance to fully characterize each device's irradiance response. The site's irradiance profile was then combined with this response to compute a site-specific global efficiency. The local irradiance profile and the device irradiance response were used to calculate the devices' global efficiency for the site, as defined in (1). This efficiency (η_{global}) is defined as the summation of the product between the device efficiency curve as a function of irradiance ($\eta(G)$) and the irradiance energy distribution across irradiance levels ($H(G)$). It serves as an indicator of the device's effective field efficiency at a given site, accounting for variations in irradiance level. However, this metric does not consider other relevant effects such as temperature, thereby isolating the influence of irradiance.

$$\eta_{\text{global}} = \sum_{G} \eta(G) \times H(G) \tag{1}$$

3. Results and Discussion

3.1. Site Irradiance Profile

The site's irradiance profile (Figure 3) presents the distribution of incident energy as a function of the global plane-of-array irradiance (GPOA). Most of the energy is concentrated in the range between 700 and 1100 W/m², with a peak around 1000 W/m², corresponding to standard test conditions (STC). However, a significant portion of the total energy occurs above this level, extending up to approximately 1500 W/m², confirming the occurrence of over-irradiance events at the measurement site. As shown in Table 1, irradiance levels above 1000 W/m² (1 sun) accounted for more than one fourth of the total received energy during the evaluated period, while extreme values exceeding 1250 W/m² represented 1.4%.

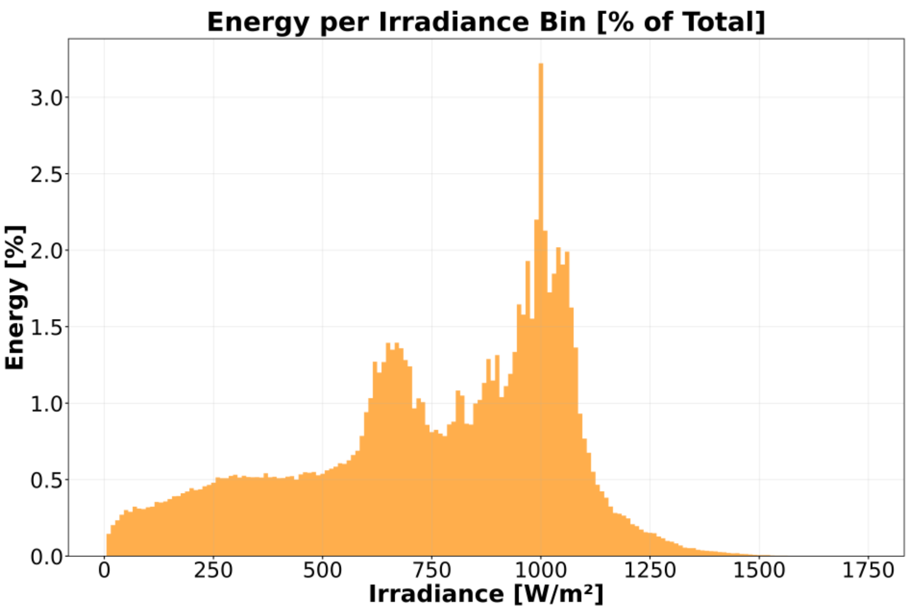

Figure 3: Plane-of-array irradiation distribution by irradiance level for a single-axis tracker at the Fotovoltaica/UFSC Research Laboratory in Florianópolis, Brazil (27.4°S, 48.4°W) during the analyzed period (March–September 2025).

Table 1: Summary of plane-of-array irradiation distribution by irradiance level for a single-axis tracker at the Fotovoltaica/UFSC Research Laboratory in Florianópolis, Brazil (27.4°S, 48.4°W) during the analyzed period (March–September 2025).

Irradiance Interval [W/m^2]	Energy Fraction [%]
0 - 250	7.1%
250 -500	12.6%
500 - 750	23.2%
750 - 1000	27.3%
1000 - 1250	24.2%
> 1250	1.4%

A comparison between the measured irradiance curve and the clear sky model (Figure 4) shows that real irradiance exceeded the theoretical model several times, particularly between 10:00 and 15:00 h, evidencing the occurrence of transient over-irradiance peaks. These peaks are characteristic of partly cloudy days, when the cloud-edge effect amplifies the direct irradiance on the module—an effect known as cloud enhancement (Gueymard, 2017). Such conditions are representative of the typical solar regime in Brazil and justify a detailed evaluation of device performance under irradiance levels exceeding 1 sun.

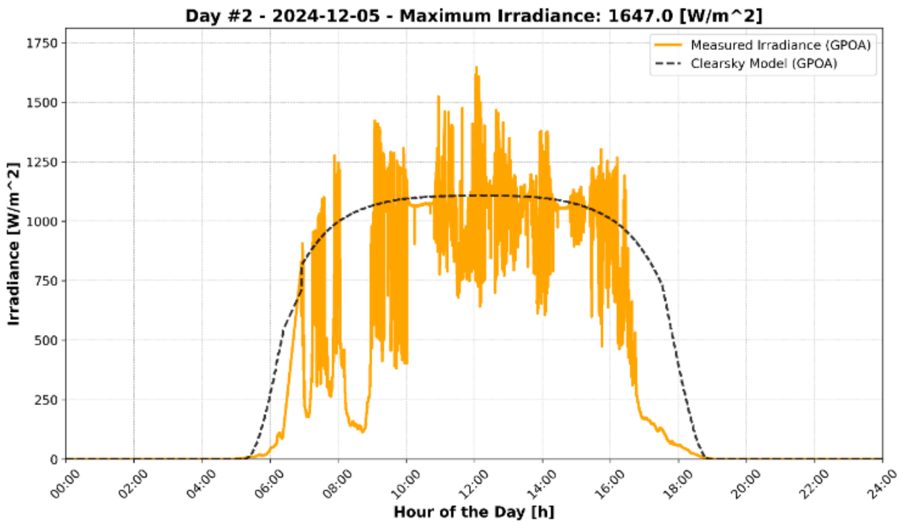

Figure 4: Time series of single-axis tracker plane-of-array irradiance on the highest-irradiance day during the study period (5 December 2024), measured at the Fotovoltaica/UFSC Research Laboratory in Florianópolis, Brazil (27.4°S, 48.4°W).

3.2. Outdoor Performance Across Irradiance Levels

Figure 5 shows the PV device STC-corrected (temperature and spectrum) efficiency as a function of plane-of-array irradiance for the two PERC samples. The PERC samples exhibited similar behavior in outdoor measurements. The efficiency corrected to 25 °C was about 21% for 300–600 W/m² and declined smoothly with increasing irradiance; the mean (black) trend line approached 18–19% at 1000 W/m². The mean values for sample 2 (Figure 5b) show irregular behavior at high irradiance levels, where fewer data points are available. This results from a smaller number of I–V curves meeting the minimum criteria for temperature correction at these irradiance levels, mainly due to their altered shape.

Figure 6 shows the corresponding fill factor (FF) versus irradiance plots. The fill factor of the PERC samples gradually decreases with increasing irradiance, from approximately 80% at low irradiance to around 60% at 1000 W/m². The decrease in FF becomes more pronounced above 700 W/m², indicating significant series-resistance effects and increasing losses at higher operating currents. In Figure 6b, a more pronounced decrease in FF can be clearly observed for sample 2, indicating higher series resistance. This also explains the reduced number of data points in the STC-corrected efficiency plot shown in Figure 5b, since the IV curve correction procedure employed is more suitable for non-degraded devices.

It is important to highlight that the observed behaviors and plot shapes correspond to a degraded sample subjected to accelerated damp-heat aging. Therefore, they do not necessarily reflect the intrinsic irradiance response of PERC cells, but also degradation effects that may have occurred, which strongly depend on the encapsulant and packaging materials used in manufacturing the devices.

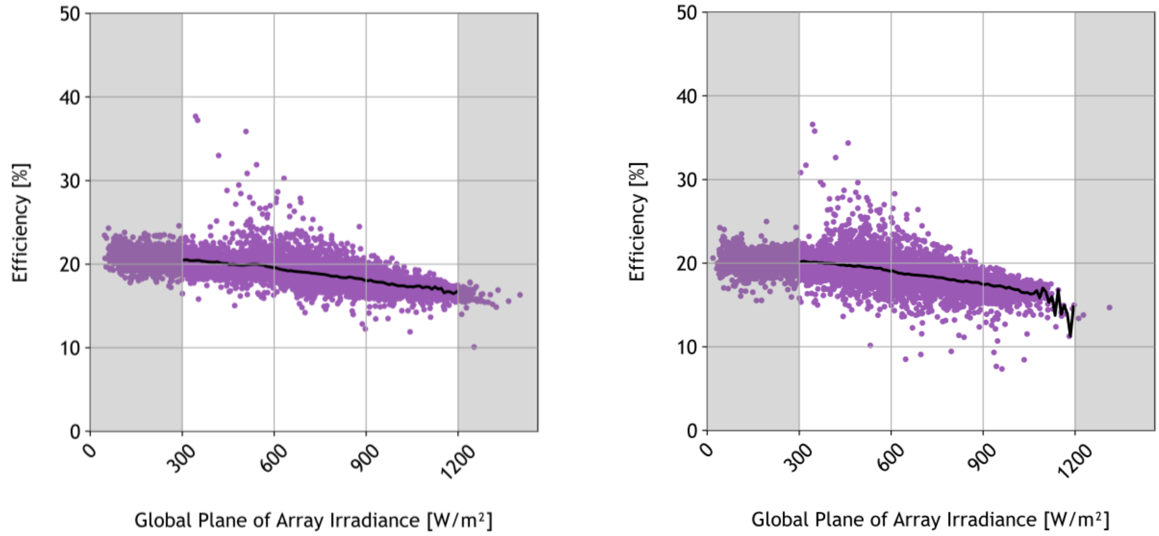

(a) (b)

Figure 5: STC-corrected efficiency as a function of irradiance for p-type PERC devices, measured outdoors at the Fotovoltaica/UFSC Research Laboratory in Florianópolis, Brazil (27.4°S, 48.4°W): (a) sample 1 and (b) sample 2.

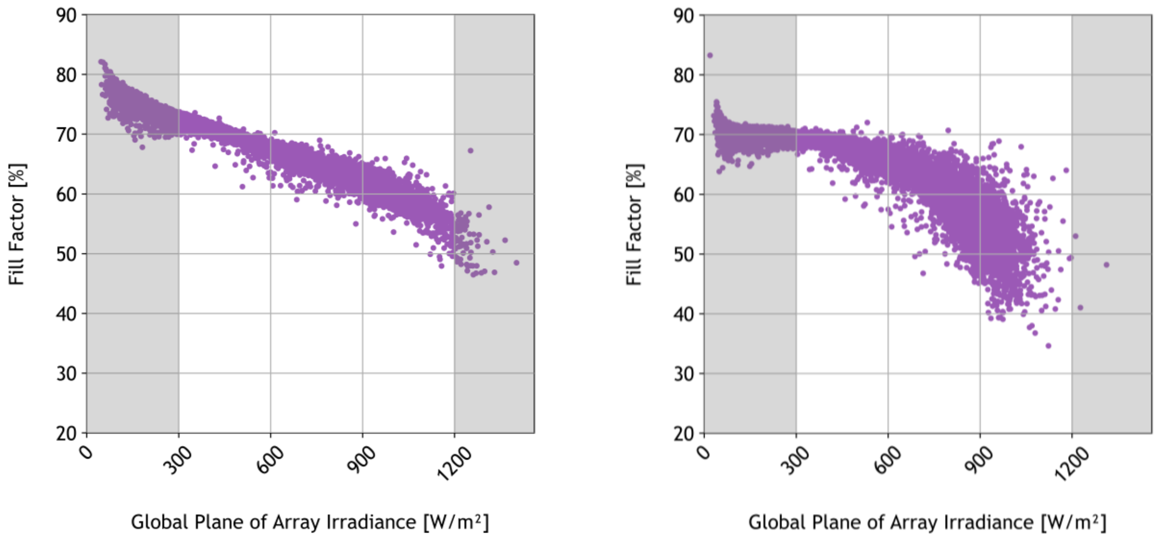

(a) (b)

Figure 6: Fill factor as a function of irradiance for the p-type PERC devices, measured outdoors at the Fotovoltaica/UFSC Research Laboratory in Florianópolis, Brazil (27.4°S, 48.4°W): (a) sample 1 and (b) sample 2.

Figure 7 shows the STC-corrected efficiency as a function of global plane-of-array irradiance for the two n-type TOPCon devices. Both samples exhibit a very stable response: the mean efficiency stays in the 21–22% range between 300 and 1,000 W/m². Data dispersion is smaller than for the p-type PERC devices, and the mean trend is nearly flat up to ≈900 W m^{-2}, with only a slight reduction at the highest irradiance levels.

Figure 8 presents the corresponding fill factor as a function of irradiance. The TOPCon samples show a gradual decrease from about 80–82% at 300 W/m² to roughly 72–74% near 1,000 W/m², i.e., a smoother decline than observed for the PERC devices. The curves of the two samples follow each other closely, indicating good reproducibility.

A direct comparison highlights that, although both technologies exhibit some efficiency and fill factor reduction with increasing irradiance, the TOPCon devices maintained a more stable behavior, with nearly constant mean efficiency and a less pronounced fill factor loss over the 300–1,000 W/m² range. Overall, the results suggest that the aged n-type TOPCon modules are less affected by high-irradiance losses than the p-type PERC devices and provide more stable performance under elevated irradiance conditions. This behavior, however, may reflect degradation from damp-heat aging rather than the cells' intrinsic irradiance response.

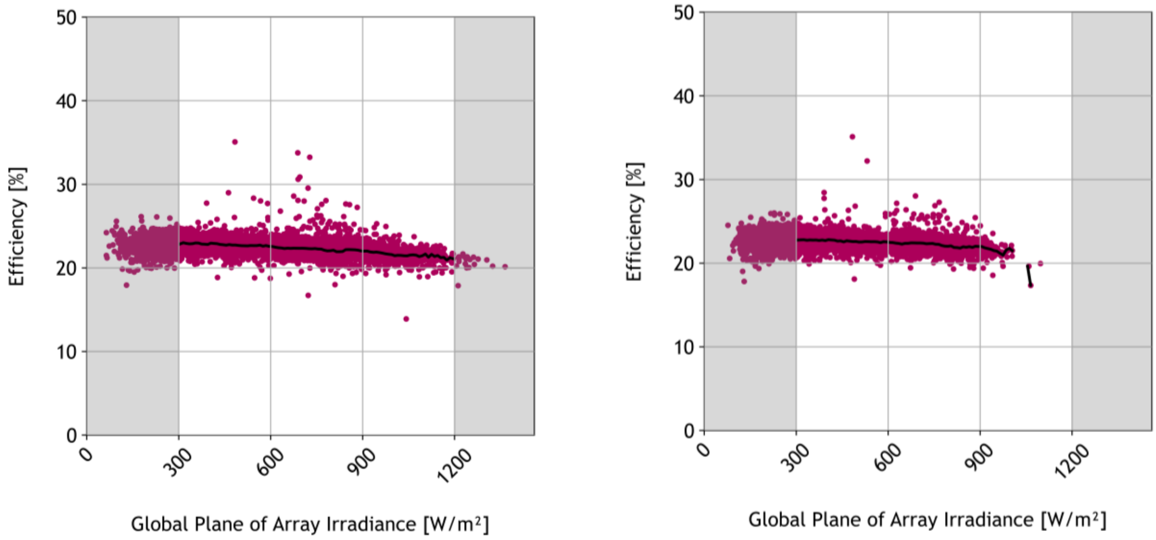

(a) (b)

Figure 7: STC-corrected efficiency as a function of irradiance for n-type TOPCon devices, measured outdoors at the Fotovoltaica/UFSC Research Laboratory in Florianópolis, Brazil (27.4°S, 48.4°W): (a) sample 3 and (b) sample 4.

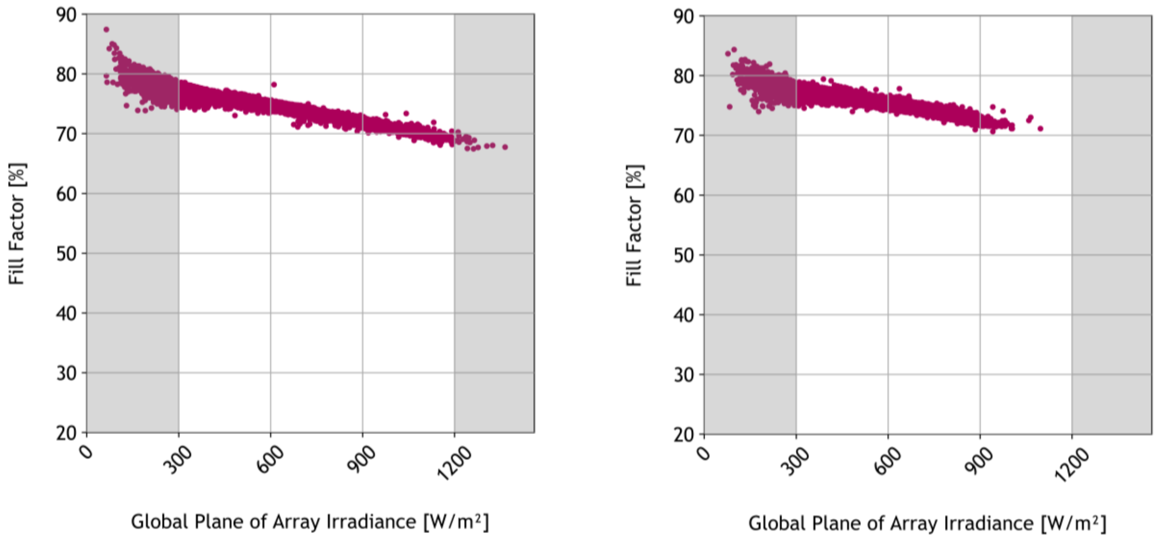

(a) (b)

Figure 8: Fill factor as a function of irradiance for the n-type TOPCon devices, measured outdoors at the Fotovoltaica/UFSC Research Laboratory in Florianópolis, Brazil (27.4°S, 48.4°W): (a) sample 3 and (b) sample 4.

3.3. Indoor Performance Under Different Illumination Levels

Figure 9 presents the STC-corrected efficiency as a function of illumination level for the p-type PERC samples, which show consistent behavior in the indoor measurements. At irradiance levels near 300 W/m², the efficiency is around 22–23% and gradually decreases with increasing irradiance, reaching about 19–20% at 1000 W/m². This nearly linear decline is consistent with internal ohmic losses which increase resistive losses at higher current levels and agrees with the extracted series resistance of 15.43 Ω·cm², which is relatively high.

Figure 10 shows the corresponding STC-corrected fill factor for the p-type PERC modules. The fill factor starts near 78% and gradually decreases to around 70% at 1000 W/m² for both samples. This systematic reduction at higher irradiance reinforces the influence of series-resistance losses and helps explain the efficiency drop observed under high illumination levels.

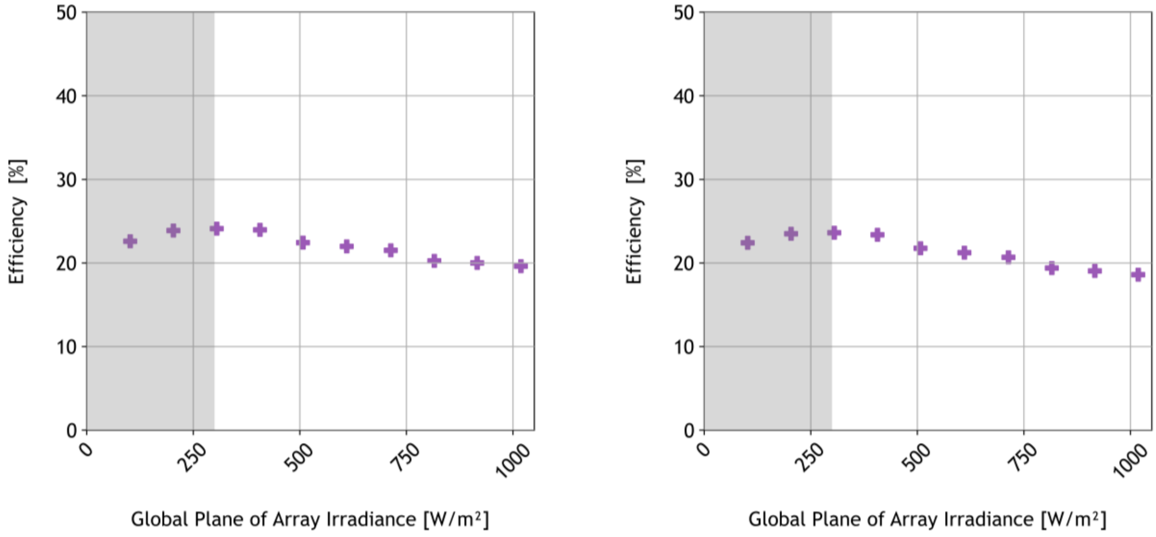

(a) (b)

Figure 9: STC-corrected efficiency as a function of illumination level for the p-type PERC devices measured under controlled conditions in the indoor solar-simulator setup at the Fotovoltaica/UFSC research lab: (a) sample 1, (b) sample 2.

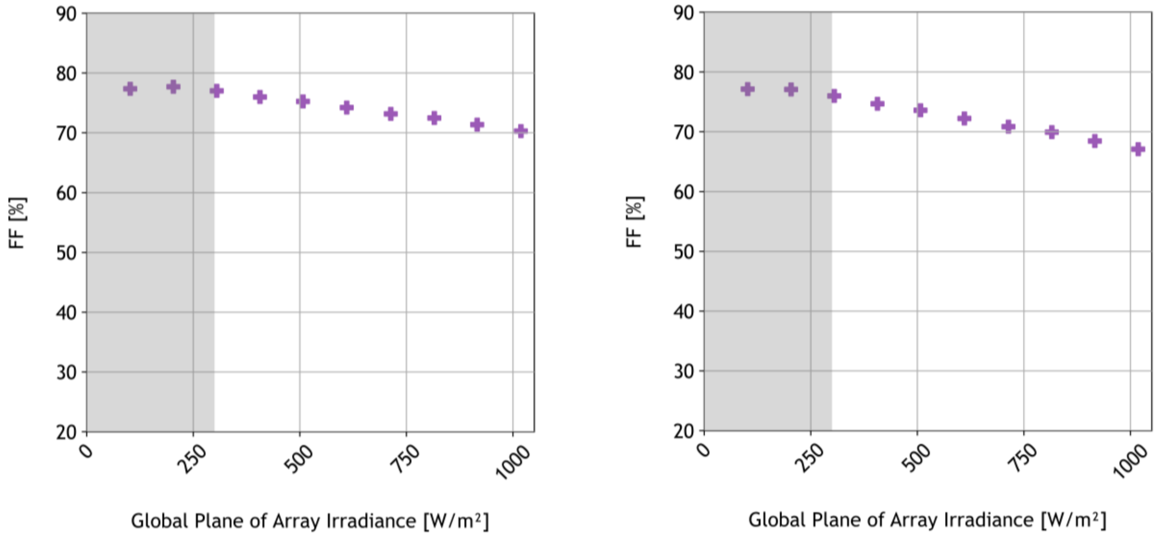

(a) (b)

Figure 10: Fill factor as a function of illumination level for the p-type PERC devices measured under controlled conditions in the indoor solar-simulator setup at the Fotovoltaica/UFSC research lab: (a) sample 1, (b) sample 2.

Figure 11 shows the STC-corrected efficiency of the n-type TOPCon samples as a function of irradiance. Both samples exhibit a very stable response: the efficiency is about 26% at 300 W/m² and decreases smoothly to approximately 23–24% at 1000 W/m². This limited variation is consistent with lower ohmic losses and agrees with the extracted series resistance of 8.01 Ω·cm², indicating better internal electrical conduction and more consistent performance at high irradiance.

Figure 12 presents the corresponding STC-corrected fill factor curves. The TOPCon samples maintain high FF values, from roughly 82% at low irradiance to about 79–80% at 1000 W/m², with only a minor decline across the tested range. The combination of high, stable efficiency and fill factor confirms the robustness of the TOPCon architecture in handling increased current while mitigating resistive losses.

Comparing both technologies under indoor conditions, both PERC and TOPCon exhibit an efficiency decrease with increasing irradiance, but with distinct magnitudes and trends. The PERC samples show a more pronounced reduction in efficiency and fill factor, consistent with their higher series resistance. In contrast, the TOPCon samples retain higher and more stable efficiency and FF, demonstrating superior electrical conduction and reduced performance degradation at high irradiance. These indoor results are consistent with the outdoor observations indicate that the aged n-type TOPCon modules experience smaller performance losses at high irradiance than the p-type PERC devices, showing more stable behavior under elevated conditions. However, this difference may be influenced by degradation from damp-heat aging rather than the intrinsic irradiance response of the cells.

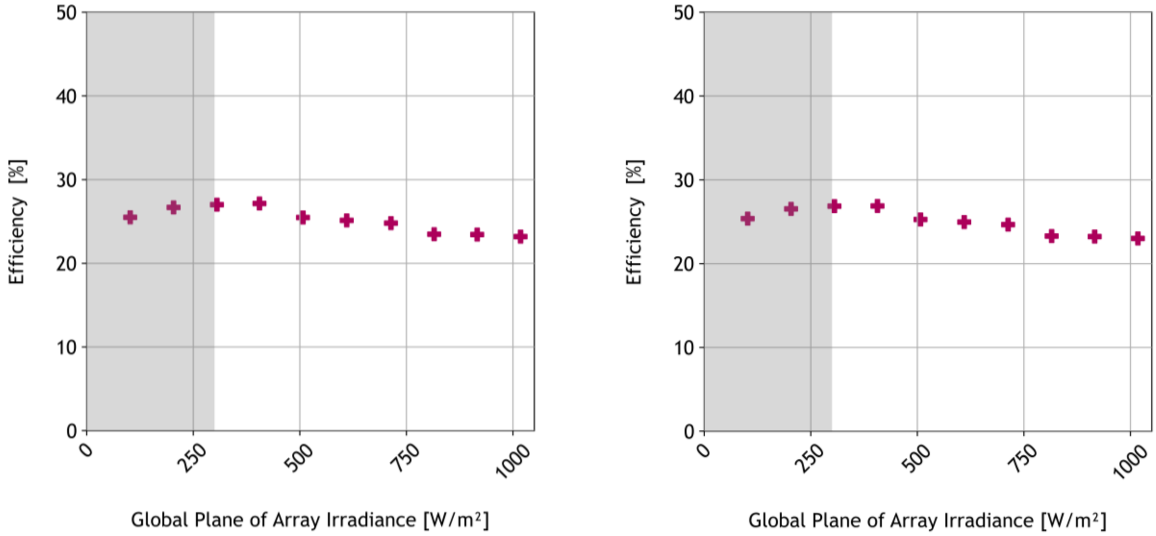

(a) (b)

Figure 11: STC-corrected efficiency as a function of illumination level for the n-type TOPCon devices measured under controlled conditions in the indoor solar-simulator setup at the Fotovoltaica/UFSC research lab: (a) sample 3, (b) sample 4.

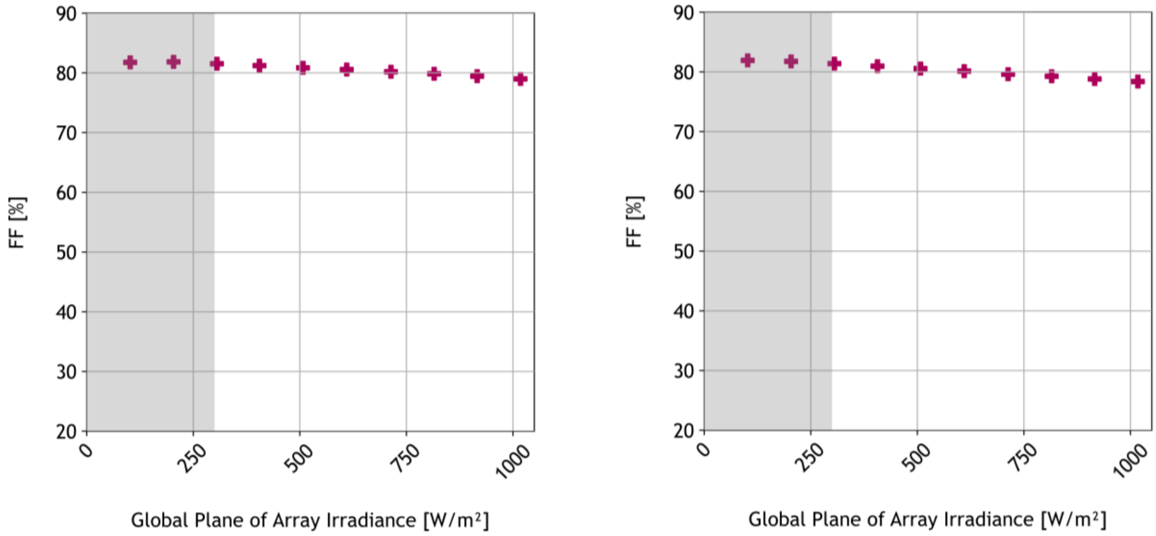

(a) (b)

Figure 12: Fill factor as a function of illumination level for the n-type TOPCon devices measured under controlled conditions in the indoor solar-simulator setup at the Fotovoltaica/UFSC research lab: (a) sample 3, (b) sample 4.

3.4. Global Efficiency

Figure 13 presents the average efficiency per irradiance bin (left axis) superimposed on the distribution of incident energy (right axis), allowing assessment of the relative contribution of each irradiance range to the overall device performance. The results show that the largest share of available energy at the site is concentrated between 700 and 1100 W/m², corresponding to approximately 60% of the total measured energy. Within this range, the main performance differences among the tested devices become evident.

Samples 1 and 2 (p-type PERC) exhibit a gradual efficiency decrease from around 600 W/m², maintaining average values near 20–22%. In contrast, samples 3 and 4 (n-type TOPCon) sustain a slightly higher and more stable efficiency across the entire analyzed range, with average values between 22–24%.

The overlap between efficiency response and energy distribution shows that most of the received energy occurs precisely within the irradiance range where the TOPCon technology maintains steadier performance, reinforcing its higher potential for global energy conversion. This combined analysis of efficiency and energy distribution can be summarized in a weighted global efficiency indicator that better represents real operating conditions, emphasizing the importance of characterizing photovoltaic devices based on their full irradiance-response profile rather than measurements under standard conditions.

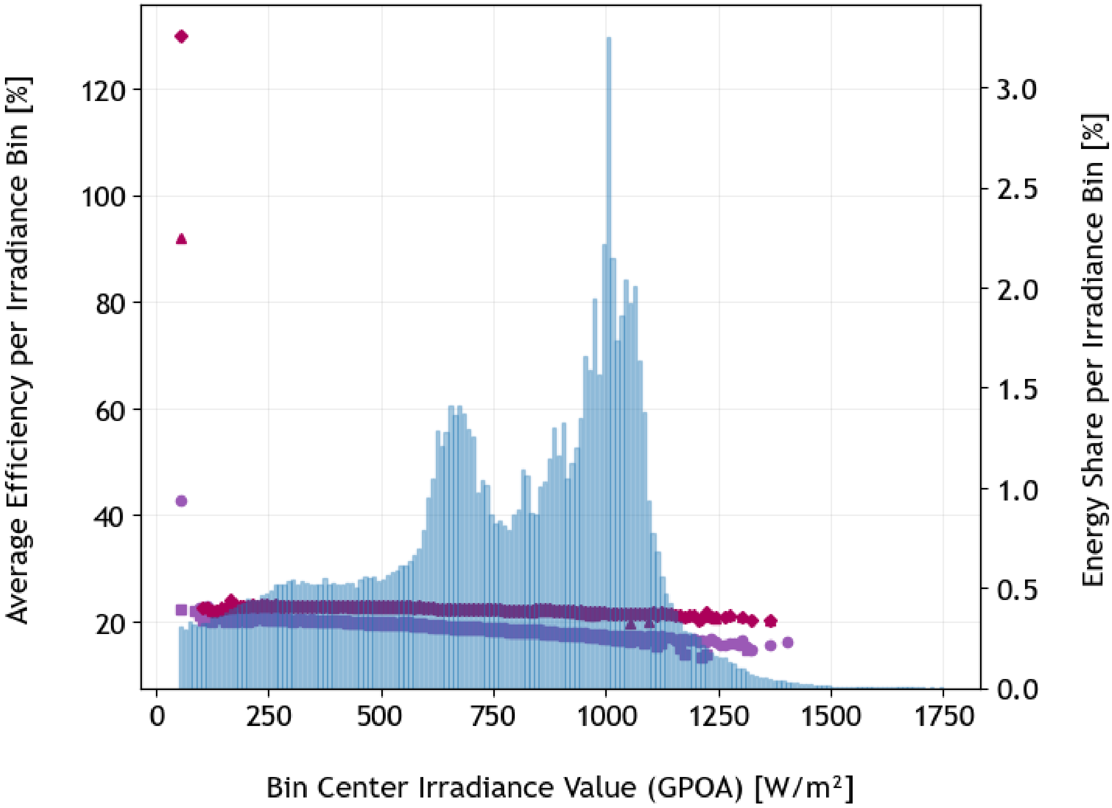

Figure 13: Average device efficiency per irradiance bin (left axis) overlaid with the plane-of-array energy distribution (right axis) for the single-axis-tracker outdoor setup at the Fotovoltaica/UFSC research lab in Florianópolis, Brazil (27.4°S, 48.4°W).

Table 2 summarizes the measured efficiencies under three distinct conditions: STC (1000 W/m²), global weighted (all irradiance levels), and beyond 1-sun (>1000 W/m²). The results show that TOPCon devices exhibit higher global efficiency compared to PERC devices, with values ranging from 19.8% to 22.4%, while PERC devices range from 17.7% to 18.7%. This difference is more pronounced than that observed under STC conditions, indicating that the enhanced high-irradiance response of TOPCon translates into a measurable energy gain for the specific climatic profile studied. When considering only the over-irradiance regime (above 1000 W/m²), TOPCon maintains average efficiencies between 20.4% and 21.4%, whereas PERC devices drop to 16.2%–17.2%, confirming their greater operational stability under intense sunlight. These results are consistent with the results presented in Figure 13, where the largest share of incident energy (700–1100 W/m²) coincides with the irradiance range in which TOPCon maintains a steadier efficiency, contributing to its higher overall energy-weighted efficiency.

Table 2: Summary of device efficiencies under STC, global weighted irradiance levels, and high-irradiance conditions (>1000 W/m²) for the single-axis-tracker outdoor setup at the Fotovoltaica/UFSC research lab in Florianópolis, Brazil (27.4°S, 48.4°W).

Efficiency Index	Irradiance Range [W/m²]	p-type PERC (sample 1)	p-type PERC (sample 2)	n-type TOPCon (sample 3)	n-type TOPCon (sample 3)
STC	1000 W/m²	17.4%	16.9%	21.5%	21.6%
Global	All	18.7%	17.7%	22.4%	19.8%
Beyond 1-sun	>1000 W/m²	17.2%	16.2%	21.4%	20.4%

From a physical standpoint, the observed differences can be primarily attributed to internal ohmic losses, which increase with higher current levels. The lower series resistance of the TOPCon devices (8.01 Ω·cm² compared to 15.43 Ω·cm² for PERC) mitigates these losses under high irradiance, leading to a higher fill factor and, consequently, improved efficiency. Additionally, more favorable temperature coefficients and better control of carrier recombination at contact interfaces may also contribute to the superior performance observed.

4. Conclusion

The results obtained from both outdoor and indoor measurements consistently show that the aged p-type PERC and n-type TOPCon samples experience efficiency reductions under high irradiance, though with different magnitudes and stability levels. Importantly, because the samples were damp-heat aged, part of the observed behavior may stem from degradation effects linked to encapsulant or packaging materials, not solely from the intrinsic characteristics of the cell technologies.

In the outdoor tests, both technologies exhibited a progressive efficiency decline above 1000 W/m², driven by increased internal resistive losses. This effect was considerably more pronounced in the p-type PERC devices, which showed larger data dispersion and a more substantial drop in fill factor. The n-type TOPCon samples, in contrast, maintained more stable efficiency and FF values, indicating greater electrical robustness under elevated irradiance levels.

The indoor measurements confirmed these trends. Under controlled thermal conditions (±1°C), the p-type PERC devices again displayed a stronger efficiency drop with increasing illumination, while the n-type TOPCon devices preserved a more consistent performance across the evaluated range. This agreement between environments reinforces the technological distinction observed in the field.

Spectral corrections were applied to ensure comparability between devices and measurement conditions. Minor discrepancies between indoor and outdoor results can be attributed to residual uncertainties in temperature correction and to moment-to-moment spectral variations inherent to field measurements.

A direct comparison of electrical parameters shows that ohmic losses are the main driver of the performance differences: the average series resistance was 15.43 Ω·cm² for PERC and 8.01 Ω·cm² for TOPCon, explaining the superior behavior of the n-type devices under high irradiance.

These findings underscore the importance of evaluating PV technologies beyond STC, especially in regions that frequently experience over-irradiance events. Aging further accentuates performance losses, as degradation in encapsulation and packaging materials can modify the electrical behavior in ways not captured by intrinsic cell characteristics alone. The results also highlight opportunities to optimize cell and module design — particularly metallization layouts and packaging strategies — to enhance performance under high-irradiance operating conditions.

Overall, the results show that the aged n-type TOPCon devices experience smaller performance losses under high irradiance than the aged p-type PERC samples, maintaining greater stability across the evaluated conditions. While part of this behavior may stem from degradation induced by damp-heat aging—rather than solely the intrinsic cell response—the combined analysis of irradiance distribution, efficiency trends, and global weighted efficiencies indicates that the evaluated TOPCon devices adapted more effectively to real operating conditions, converting this robustness into higher overall operating efficiency.

5. Acknowledgements

This research was carried out within the scope of the activities of the National Institute for Technological Development of Photovoltaic Solar Energy Applications, INCT-DAESF, CNPq/MCTI/Brazil, Process 408486/2024-4. The authors acknowledge the financial support provided by SHELL through projects 22076-4 and 22717-3 within the framework of the Research, Development and Innovation (RD&I) program of the Brazilian National Agency of Petroleum, Natural Gas and Biofuels (ANP). The authors are also grateful to Brametal for donating the tracker used as the experimental platform, and to Romiotto and EKO for the development and supply of the measurement system, and to BYD for donating the minimodules employed in the experiments. In addition, the authors would like to thank their colleagues at the Fotovoltaica/UFSC laboratory who, although not directly involved in this research, played a crucial role in the design, installation, and maintenance of the systems used throughout the study.

6. References

Braga, M., De Oliveira, A.K.V., Burnham, L., Dittmann, S., Gottschalg, R., Betts, T., Rodriguez-Gallegos, C.D., Reindl, T., Ruther, R., 2020. Solar Over-Irradiance Events: Preliminary Results from a Global Study, in: Conference Record of the IEEE Photovoltaic Specialists Conference. Institute of Electrical and Electronics Engineers Inc., pp. 2764–2770. https://doi.org/10.1109/PVSC45281.2020.9300868

Braga, M., Sérgio, L.A.Z., Pires, A.M., Ribeiro, M.L.C., Rüther, R., 2024. Resultados Preliminares para Dispositivos de Perovskita em Condições Reais e Extremas de Operação - Um Passo Fundamental Rumo a Aplicações Práticas. Presented at the Anais CBENS 2024. https://doi.org/10.59627/cbens.2024.2536

Gueymard, C.A., 2017. Cloud and albedo enhancement impacts on solar irradiance using high-frequency measurements from thermopile and photodiode radiometers. Part 1: Impacts on global horizontal irradiance. Solar Energy 153, 755–765. https://doi.org/10.1016/j.solener.2017.05.004

IEC, 2021a. IEC 61215-1 - Terrestrial photovoltaic (PV) modules – Design qualification and type approval – Part 1: Test requirements.

IEC, 2021b. IEC 60891:2021 - Photovoltaic devices - Procedures for temperature and irradiance corrections to measured I-V characteristics.

IEC, 2020. IEC 60904-9:2020 - Photovoltaic devices—Part 9: Classification of solar simulator characteristics.

Martins, G.L., Mantelli, S.L., Rüther, R., 2022. Evaluating the performance of radiometers for solar overirradiance events. Solar Energy 231, 47–56. https://doi.org/10.1016/j.solener.2021.11.050

Nascimento, L.R., de Souza Viana, T., Campos, R.A., Rüther, R., 2019. Extreme solar overirradiance events: Occurrence and impacts on utility-scale photovoltaic power plants in Brazil. Solar Energy 186, 370–381. https://doi.org/10.1016/j.solener.2019.05.008

NREL, 2025. Best Research-Cell Efficiency Chart [WWW Document]. URL https://www.nrel.gov/pv/interactive-cell-efficiency.html (accessed 10.20.25).

Queiroz, L.M., Sturm, L.-M.C., Braga, M., Rüther, R., 2022. Optimization of the number of busbars in crystalline silicon solar cells. Presented at the Anais CBENS 2024. https://doi.org/10.59627/cbens.2022.1209

Shockley, W., Queisser, H.J., 1961. Detailed balance limit of efficiency of p-n junction solar cells. Journal of Applied Physics 32, 510–519. https://doi.org/10.1063/1.1736034